A Decoupling and Matching Network With Harmonic Suppression for MIMO Antennas

Zhang, Yiming; Zhang, Shuai

A Decoupling and Matching Network With Harmonic Suppression for MIMO Antennas

Yi-Ming Zhang, Shuai Zhang

Antennas, Propagation and Millimeter-wave Systems (APMS) Section, Department of Electronic Systems, Aalborg University, Aalborg 9220, Denmark

{yiming, sz}@es.aau.dk

Abstract—This article presents a decoupling and impedance matching network with harmonic suppression for two-element antenna arrays, including a resistor-loaded decoupling part and a slotline-based impedance matching and harmonic suppression part. By integrating with the proposed network, the mutual coupling between the elements at the center frequency can be well suppressed. Moreover, the second-order harmonic is also suppressed to a low level. For verification purposes, a 2×2 dual-polarized antenna array centered at 3.5 GHz is employed and integrated with the proposed networks. A 3-D model is constructed and full-wave simulations are carried out. The results denote that the strongest in-band mutual coupling is suppressed from -16.6 dB to less than -25 dB, and a good out-of-band rejection level up to 10 GHz is obtained.

Index Terms—MIMO antennas, decoupling, harmonic.

I. INTRODUCTION

As a key challenge of MIMO antenna systems, mutual coupling suppression between antenna elements has attracted increasing attention [1], [2]. In terms of communication capacity and linearity of power amplifiers, the influence of the mutual coupling among antenna elements on the performance of systems is significant.

In the past decade, many efforts have been devoted to dealing with the coupling issue, such as electromagnetic bandgap structure [3], decoupling metasurface [4], defected ground [5], and scatter-loaded scheme [6]. Most of these approaches need additional space for placing the decoupling structures, at the cost of large element distances, high profile, or bulky system sizes. Network-based decoupling is an alternative for compactly positioned antennas since it is operated at the feeding layer and no additional structure is added at the radiating layer, such as the methods reported in [7]-[10]. These schemes enable well-established in-band decoupling for antenna arrays. However, the spurious level or out-of-band rejection, especially the harmonic suppression, is not involved. As for the out-of-band spurious level, it might raise after decoupling [7], which would increase the burden of the subsequent filtering module from the entire system point of view.

In this work, a compact decoupling network integrated with a slotline-based impedance matching and harmonic suppression structure is proposed for MIMO antennas. Theoretical analysis is carried out to investigate the responses. A design example consisting of a 2×2 dual-polarized antenna array and the proposed decoupling network is further developed to verify the performance. The full-wave simulated results denote that high levels of in-band mutual coupling suppression and out-of-band rejection are both obtained.
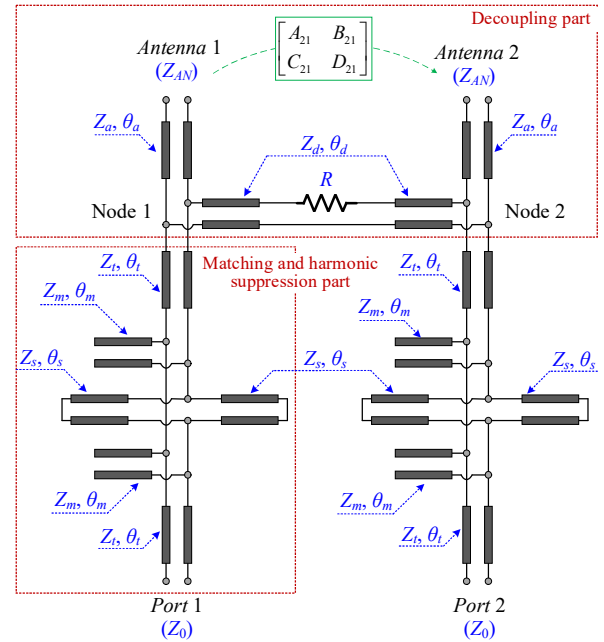
Fig. 1. Equivalent circuit model of the proposed decoupling network for two-element array.

II. ANALYSIS OF THE PROPOSED SCHEME

Fig. 1 illustrates the equivalent circuit model of the proposed decoupling network for a two-element array. The network includes two layers, where the first layer is a resistor-loaded decoupling part, and the second one is a slotline-based impedance matching and harmonic suppression part. With the proposed scheme, the coupling between the two antennas can be well suppressed. Moreover, the spurious is also suppressed among a wide frequency band. Next, the decoupling and harmonic suppression performance will be studied using transmission-line theory.
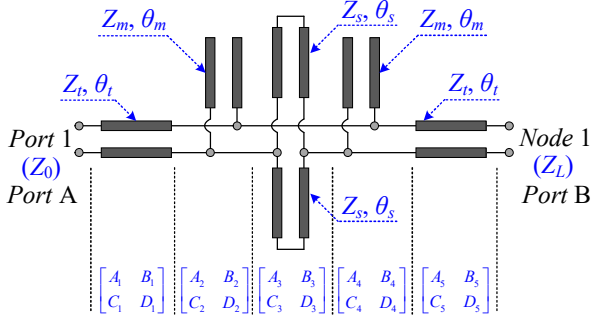
Fig. 2. Equivalent circuit of the matching and harmonic suppression part of the proposed scheme.

The transmission matrix from Node 1 to Node 2 through the path of antenna coupling can be expressed as [11]

$$\begin{bmatrix} a_1 & b_1 \\ c_1 & d_1 \end{bmatrix} = \begin{bmatrix} \cos\theta_a & jZ_a\sin\theta_a \\ \dfrac{j\sin\theta_a}{Z_a} & \cos\theta_a \end{bmatrix} \begin{bmatrix} A_{21} & B_{21} \\ C_{21} & D_{21} \end{bmatrix}$$
$$\times \begin{bmatrix} \cos\theta_a & jZ_a\sin\theta_a \\ \dfrac{j\sin\theta_a}{Z_a} & \cos\theta_a \end{bmatrix} \quad (1)$$

On the other hand, the transmission matrix from Node 1 to Node 2 through the resistor-loaded bridge can be given as

$$\begin{bmatrix} a_2 & b_2 \\ c_2 & d_2 \end{bmatrix} = \begin{bmatrix} \cos\theta_d & jZ_d\sin\theta_d \\ \dfrac{j\sin\theta_d}{Z_d} & \cos\theta_d \end{bmatrix} \begin{bmatrix} 1 & R \\ 0 & 1 \end{bmatrix}$$
$$\times \begin{bmatrix} \cos\theta_d & jZ_d\sin\theta_d \\ \dfrac{j\sin\theta_d}{Z_d} & \cos\theta_d \end{bmatrix} \quad (2)$$

Based on (1) and (2), the mutual admittance from Node 1 to Node 2 can be expressed as

$$Y_{21} = -\frac{1}{b_1} - \frac{1}{b_2} \quad (3)$$

For decoupling purposes, we have

$$Y_{21} = 0 \quad (4)$$

Based on the above discussion, the values of Z_a, θ_a, Z_d, θ_d, and R can be determined.

As shown in Fig. 1, the second part of the proposed scheme is a matching network with harmonic suppression. In this case, the following values are employed that $\theta_t = \theta_m = \pi/8$, $\theta_s = \pi/4$ at the operating frequency f_0. Fig. 2 shows the two-port equivalent circuit of the second part of the scheme.

Based on the circuit plotted in Fig. 2, the transmission matrix of the two-port circuit model is formulated as

$$\begin{bmatrix} a_3 & b_3 \\ c_3 & d_3 \end{bmatrix} = \begin{bmatrix} A_1 & B_1 \\ C_1 & D_1 \end{bmatrix} \begin{bmatrix} A_2 & B_2 \\ C_2 & D_2 \end{bmatrix} \begin{bmatrix} A_3 & B_3 \\ C_3 & D_3 \end{bmatrix}$$
$$\times \begin{bmatrix} A_4 & B_4 \\ C_4 & D_4 \end{bmatrix} \begin{bmatrix} A_5 & B_5 \\ C_5 & D_5 \end{bmatrix} \quad (5)$$
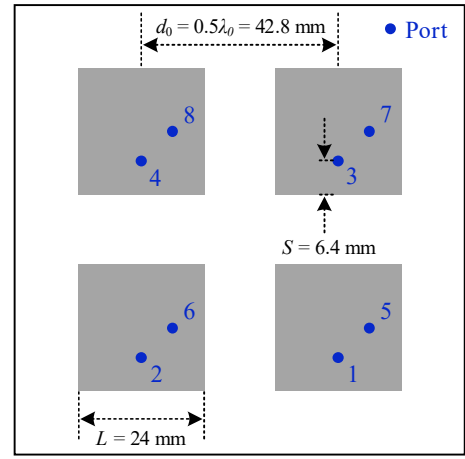
Fig. 3. Configuration of the 2×2 patch antenna array.

Subsequently, the S parameters of the two-port network shown in Fig. 2 is derived, given as [12]

$$S_{A,A} = \frac{a_3 Z_L + b_3 - c_3 Z_0 Z_L - d_3 Z_0}{a_3 Z_L + b_3 + c_3 Z_0 Z_L + d_3 Z_0} \quad (6a)$$

$$S_{B,A} = \frac{2\sqrt{Z_0 R_L}}{a_3 Z_L + b_3 + c_3 Z_0 Z_L + d_3 Z_0} \quad (6b)$$

where R_L is the real part of the load impedance Z_L seen looking into the antenna at Node 1. It can be readily derived that with the given values of $\theta_t = \theta_m = \pi/8$, $\theta_s = \pi/4$, the following result given in (7) always holds. This is independent of the values of the characteristic impedance of the transmission lines.

$$S_{B,A}\Big|_{f=2f_0} = 0 \quad (7)$$

This implies that the second-order harmonic can be well suppressed. Further, for impedance matching purposes, it is required that

$$S_{A,A}\Big|_{f_0} = 0 \quad (8)$$

With the given condition of (8), the rest values of the parameters shown in Fig. 2 will be determined.

In this section, the proposed decoupling scheme is theoretically analyzed, and the parameters can be determined by (1)-(8) under the conditions of decoupling and harmonic suppression. Next, a design example will be developed to further verify the performance of the presented configuration.

III. A DESIGN EXAMPLE

In this section, a dual-polarized 2×2 patch antenna array is utilized as the study case. The array configuration is illustrated in Fig. 3, where the decoupling network is positioned on the bottom layer of Substrate 3. Considering that the mutual coupling between cross-polarized ports is
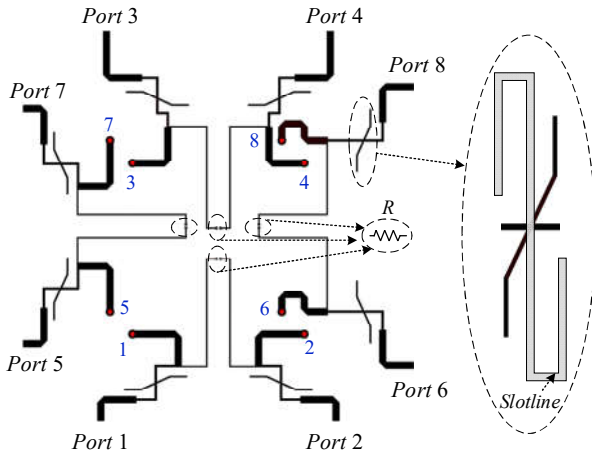
Fig. 4. Layout of the proposed decoupling network for the 2×2 array.

(a)

(b)

(c)

Fig. 5. Simulated S parameters of the decoupled 2×2 dual-polarized array. (a) $S_{1,1}$. (b) $S_{2,1}$ and $S_{3,1}$. (c) $S_{5,1}$ and $S_{6,1}$.

weak enough, there is no direct decoupling operation for the cross-polarized ports. Besides, the E-plane coupling between co-polarized ports is also at a very low level in the proposed 2×2 antenna array. Therefore, it is better to do nothing on the E-plane coupling, and the decoupling networks are only loaded between H-plane coupled ports. By following the derivation carried out in Section II, the values of parameters of the decoupling and harmonic suppression network can be determined theoretically, which are: Z_t = 94.3 Ω, Z_s = 88 Ω, Z_m = 110.1 Ω, Z_d = 50 Ω, Z_a = 50 Ω, θ_t = 22.5°, θ_s = 45°, θ_m = 22.5°, θ_a = 154.2°, θ_d = 235.7°, R = 470 Ω. By using full-wave simulated optimization, the final layout of the network is determined, as plotted in Fig. 4. The performance of the developed 2×2 antenna array is verified by using full-wave simulations.

Fig. 5 depicts the S parameters of the decoupled antenna array, where port 1 is selected as the representative port. For comparison purposes, the results of the array without decoupling are also provided. It is seen from Fig. 5(a) that the fraction bandwidth is improved from 6% to 8.7%. The H-plane coupling between co-polarized ports, i.e. $S_{2,1}$, is suppressed from -16.6 dB to less than -30 dB around the center frequency 3.5 GHz, as described in Fig. 5(b). As mentioned before, although there is no direct decoupling operation between E-plane coupled co-polarized ports, the coupling, i.e. $S_{3,1}$, is also decreased from -25 dB to -27.5 dB around the center frequency. The coupling level between cross-polarized ports is kept at a very low level, as shown in Fig. 5(c) and as expected.

Illustrated in Fig. 6 is the reflection coefficient at port 1 among a wide frequency band to show the out-of-band rejection level. The result denotes that the second-order harmonic around 8 GHz is well suppressed after integrating with the proposed decoupling network. The out-of-band magnitude of $S_{1,1}$ is higher than -2.1 dB up to 10 GHz. the far-field radiation patterns are given in Fig. 7. The results of the decoupled array are close to the ones of the array without decoupling, except a small insertion loss.
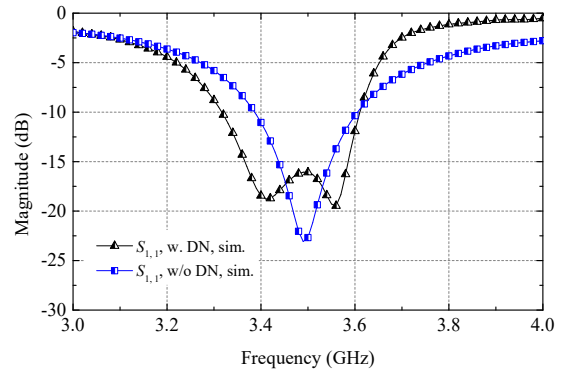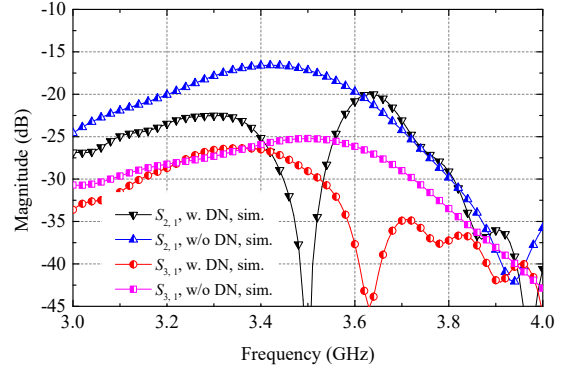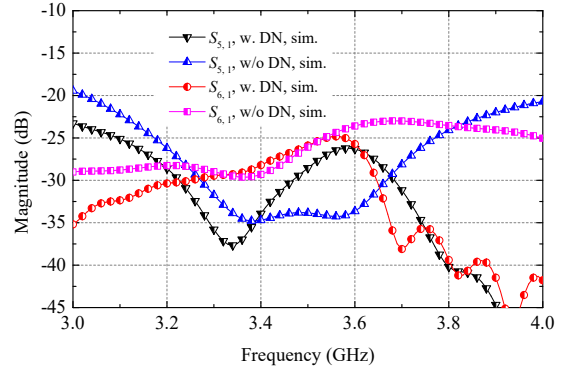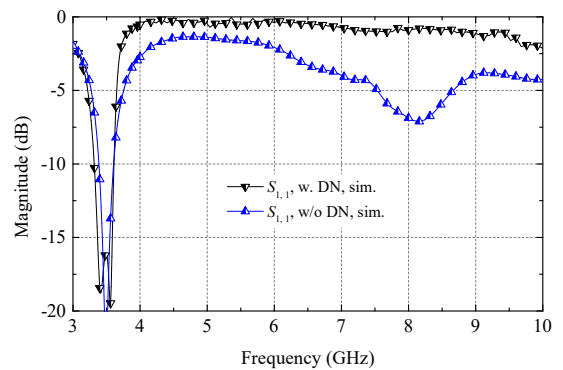
Fig. 6. Simulated $S_{1,1}$ of the array among a wide frequency band.
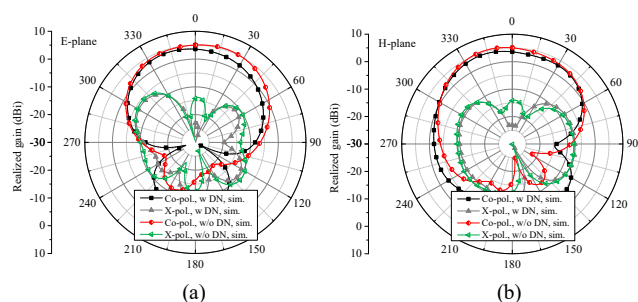
Fig. 7. Simulated radiation patterns of the 2×2 array when port 1 is excited. (a) E plane. (b) H plane.

TABLE I
COMPARISONS BETWEEN THE PROPOSED DECOUPLING SCHEME AND SOME RECENTLY PUBLISHED WORKS

Ref.	Array configuration	Out-of-band rejection	Rejection band	Out-of-band $S_{1,1}$
[3]	Single-polarized 1×2	No	/	< -7 dB
[4]	Single-polarized 1×2	No	/	< -6 dB
[5]	Single-polarized 1×2	No	/	Not given
[6]	Single-polarized 1×2	No	/	Not given
[7]	Dual-polarized 4×4	No	/	< -10 dB
[8]	Single-polarized 1×2	No	/	Not given
[9]	Single-polarized 1×2	No	/	Not given
[10]	Single-polarized 1×2, 1×3	No	/	Not given
This work	Dual-polarized 2×2	Yes	$2.8f_0$	> -2.1 dB

For comparison purposes, some recently published decoupling methods are summarized and listed in Table I. It is seen that most of these works are powerful for single polarized antenna arrays. Moreover, the spurious signals within out of band are not suppressed. As for the proposed scheme, the harmonics of up to 2.8 times the center frequency f_0 has been well-suppressed. The proposed method features low profile, low loss, and can be used for dual-polarized array configurations.

IV. CONCLUSION

A compact decoupling network is proposed and studied in this article for MIMO antennas. The network consists of a resistor-loaded decoupling part and a slotline-based matching and harmonic suppression part. A numerical derivation is proposed by using the transmission-line theory, to determine the values of the parameters of the network. A design example is further developed for verification purposes. More detailed, a 2×2 dual-polarized patch antenna array is used and integrated with the proposed network. Full-wave simulations show that the well-designed mutual coupling suppression at the operating frequency is obtained, with a second-order harmonic suppression.

REFERENCES

[1] X. Chen, S. Zhang, and Q. Li, "A review of mutual coupling in MIMO systems." *IEEE Access*, vol. 6, pp. 24706-24719, 2018.

[2] L. Savy and M. Lesturgie, "Coupling effects in MIMO phased array," in *Proc. IEEE Radar Conf.* (*RadarConf*), Philadelphia, PA, USA, May 2016, pp. 1–6.

[3] X. Tan, W. Wang, Y. Wu, Y. Liu, and A. A. Kishk, "Enhancing isolation in dual-band meander-line multiple antenna by employing split EBG structure," *IEEE Trans. Antennas Propag.*, vol. 67, no. 4, pp. 2769-2774, Apr. 2019.

[4] F. Liu, J. Guo, L. Zhao, G.-L. Huang, Y. Li, and Y. Yin, "Dual-band metasurface-based decoupling method for two closely packed dual-band antennas," *IEEE Trans. Antennas Propag.*, vol. 68, no. 1, pp. 552-557, Jan. 2020.

[5] D. Gao, Z.-X. Gao, S.-D. Fu, X. Quan, and P. Chen, "A novel slot-array defected ground structure for decoupling microstrip antenna array," *IEEE Trans. Antennas Propag.*, 2020. DOI: 10.1109/TAP.2020.2992881

[6] X. Yu, and H. Xin, "Direction-of-arrival estimation enhancement for closely spaced electrically small antenna array," *IEEE Trans. Microw. Theory Tech.*, vol. 66, no. 1, pp. 477-484, Jan. 2018.

[7] Y.-M. Zhang, S. Zhang, J.-L. Li, and G. F. Pedersen, "A transmission-line-based decoupling method for MIMO antenna arrays," *IEEE Trans. Antennas Propag.*, vol. 67, no. 5, pp. 3117-3131, May 2019.

[8] C.-H. Wu, C.-L. Chiu, and T.-G. Ma, "Very compact fully lumped decoupling network for a coupled two-element array," *IEEE Antennas Wireless Propag. Lett.*, vol. 15, pp. 158-161, 2016.

[9] H. Meng and K.-L. Wu, "An LC decoupling network for two antennas working at low frequencies," *IEEE Trans. Microw. Theory Techn.*, vol. 65, no. 7, pp. 2321–2329, Jul. 2017.

[10] M. Li, L. Jiang, and K. L. Yeung, "Novel and efficient parasitic decoupling network for closely coupled antennas," *IEEE Trans. Antennas Propag.*, vol. 67, no. 6, pp. 3574-3585, Jun. 2019.

[11] D. M. Pozar, "Microwave network analysis," in *Microwave Engineering*, 4th ed. Hoboken, NJ, USA: Wiley, 2012, ch. 4, pp. 188-194.

[12] D. A. Frickey, "Conversions between S, Z, Y, H, ABCD, and T parameters which are valid for complex source and load impedances," *IEEE Trans. Microw. Theory Tech.*, vol. 42, no. 2, pp. 205-211, Feb. 1994.